CCFE
CULHAM CENTRE FOR FUSION ENERGY

UK Atomic Energy Authority

UKAEA-CCFE-PR(19)56

Max Boleininger and Sergei L. Dudarev

Continuum model for the core of a straight mixed dislocation

Continuum model for the core of a straight mixed dislocation

Max Boleininger and Sergei L. Dudarev

This is a preprint of a paper submitted for publication in
Physical Review Materials

A continuum model for the core of a straight mixed dislocation.

Max Boleininger* and Sergei L. Dudarev†
CCFE, Culham Science Centre, UK Atomic Energy Authority, Abingdon, Oxfordshire OX14 3DB, United Kingdom
(Dated: May 3, 2019)

Linear elasticity theory predicts a divergent strain field at the dislocation core, resulting from the continuum approximation breaking down at the atomic scale. We introduce a minimum model that includes elastic interactions and discrete lattice periodicity, and derive a set of equations that treat the core of an edge dislocation from a solely geometric perspective. We find an analytical formula for the displacement field of an arbitrary straight mixed dislocation and predict that the dislocation core widens as the screw character becomes more dominant, in qualitative and quantitative agreement with atomistic simulations of mixed dislocations in tungsten. The theory is based on a continuum form of the multistring Frenkel-Kontorova model, and on the fact that a nearest neighbor model captures to a substantial degree the part played by lattice discreteness; thus, we circumvent the need to use adjustable parameters in the treatment of a dislocation core.

I. INTRODUCTION

Linear elasticity theory provides a mathematically powerful description of how a crystalline material responds to stresses resulting from either applied external forces or from internal sources, for example lattice defects. Linear elasticity theory is valid under the assumption that interatomic interactions are harmonic to the lowest order. The linear elastic Green's function method enables a straightforward evaluation of elastic strain at any point inside the material for arbitrary tractions or displacement boundary conditions at the bounding surface. In this picture, dislocations are the carriers of plastic strain, acting as sources for elastic Green's function solutions in the form of boundary conditions defined at slip planes [1].

However, the question about exactly *how* the plastic strain should be defined to reflect the real atomic configuration in the core of a dislocation lies outside the realm of linear elasticity. Textbook models of dislocations [2] follow Volterra [3] and state that a plastically slipped area, associated with a dislocation, ends abruptly inside the crystal, leading to strain that is entirely localized at the dislocation line in a delta-function-like form. An unfortunate consequence of this approximation is that elastic strain and stress fields are singular. They diverge at the dislocation line, and this gives rise to ill-defined energies and forces.

Several approaches have been developed to address this point. In methods based on the Peierls-Nabarro model [4–7], the plastic strain spreads out as a consequence of non-linear interactions across the slipped surface. The resulting methods offer highly accurate predictions of dislocation core properties, but solving the models often proves challenging [8–11]. Other approaches regularize the singular plastic strain using a convolution of it with an isotropic non-singular function [12, 13]. The resulting strain and stress fields can be computed analytically, but the atomic positions and lattice strains may not be accurate in the dislocation core region.

The objective of this study is to present a first-principles continuum model for the dislocation core in a body-centered-cubic (bcc) lattice. The resulting model is analytically tractable and offers a physical insight into the microscopic structure of the core region of a dislocation, combining the Peierls-Nabarro and regularization approaches.

Starting from a simplified description of interatomic bonding in the context of a discrete model, we relate the functional form of the plastic strain directly to elastic strain through a boundary value problem. By asserting that the atomic model is equivalent to linear elasticity theory far away from the dislocation core where the continuum approximation applies, we are able to eliminate the free parameters of the discrete model and arrive at something akin to a lowest-order description of the non-singular edge dislocation core. The derivation of the model relates the multistring Frenkel-Kontorova model [14], the Lubarda-Markenscoff variable core dislocation theory [15, 16], and - naturally - the Peierls-Nabarro and linear elasticity treatments into an internally consistent picture. By virtue of its simplicity, we are able to investigate the model analytically, and find an exact solution for the displacement field of a straight mixed dislocation.

We do not attempt to derive a continuum model for the bcc screw dislocation core, as the first principles studies [17–19] show no appreciable spreading of the plastic strain over any slip plane, other than possibly during the migration process. The singular Volterra description of the displacement field therefore appears adequate, with the caveat that the core energy remains ill-defined. It would be appropriate to note other approaches to regularizing the dislocation core energy [20–23].

In Sec. II we present a derivation of the boundary value problem for a mixed dislocation with a curved glide surface. An analytical expression for the displacement field of a straight mixed dislocation is given in Sec. III, pre-

* max.boleininger@ukaea.uk
† sergei.dudarev@ukaea.uk

dicting that the edge dislocation core widens as the screw character becomes more significant. In Sec. IV we present a correction that takes into account the finite distance between atomic rows at the opposite sides of the glide surface. In Sec. V the analytical expression for the strain field is compared to results derived from atomistic simulations of mixed $a/2[111](10\bar{1})$ dislocations in bcc tungsten. The resulting theory is able to predict the variation of strain in the dislocation core and the width of the core in agreement with molecular dynamics simulations, offering an analytical non-singular description of the core of an arbitrary mixed dislocation free from adjustable parameters.

II. A CONTINUUM MODEL FOR THE CORE OF A DISLOCATION IN BCC LATTICE

Below we introduce the multistring Frenkel-Kontorova [14] (MSFK) model, which provides a simplified description of interatomic bonding in a crystal lattice. The MSFK model describes the periodicity of the lattice in a mean-field picture: the motion of atoms is constrained to a chosen direction, with atomic interactions modelled by an effective pairwise periodic potential. In figurative terms, we consider rows of atoms like beads threaded on strings, trying to arrange themselves under the influence of mutual attraction and repulsion. By virtue of its simplicity, the MSFK model lends itself well to analytical studies, including the investigation of dislocation core properties. In the past it was applied to the investigation of structure and mobility of screw dislocations [24–26], small defects of interstitial type [14, 27, 28] and, more recently, edge dislocations [29].

However, as atomic motion is constrained along one direction only, the MSFK model is conceptually incompatible with elasticity theory, where the medium is free to deform in any direction. We shall therefore use the MSFK description only for the plastically slipped surface while treating the elastic field of the dislocation in the general linear elasticity approximation.

Consider an infinitely extended crystal lattice, containing a dislocation with Burgers vector $\boldsymbol{b}$, which here without the loss of generality is chosen to point in the Cartesian direction $\hat{\boldsymbol{z}}$. Atoms in the lattice are spatially partitioned along strings collinear with the Burgers vector. Atomic positions $\boldsymbol{r}_{n,\boldsymbol{j}}$ are indexed by their position n within a string and by the vector-valued index $\boldsymbol{j}$ denoting the location of a string in a plane orthogonal to the Burgers vector. The adjacent strings are offset by the neighbor vectors $\boldsymbol{h}$, see Fig. 1 for illustration. The MSFK Lagrangian is then given by [14]:

$$\mathcal{L} = \sum_{\boldsymbol{j}} \sum_{n=-\infty}^{\infty} \left[\frac{m\dot{z}_{n,\boldsymbol{j}}^2}{2} - \frac{\alpha}{2} \left(z_{n+1,\boldsymbol{j}} - z_{n,\boldsymbol{j}} - b \right)^2 \right] - \frac{m\omega^2 b^2}{2\pi^2} \sum_{\boldsymbol{j},\boldsymbol{h}} \sum_{n=-\infty}^{\infty} \sin^2 \left[\frac{\pi}{b} \left(z_{n,\boldsymbol{j}} - z_{n,\boldsymbol{j}+\boldsymbol{h}} \right) \right], \tag{1}$$

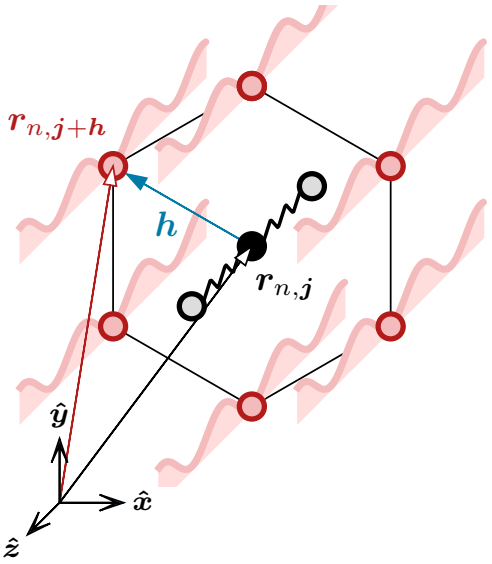

FIG. 1. Local bonding environment of an atom in the multistring Frenkel-Kontorova model. The atoms is at $\boldsymbol{r}_{\boldsymbol{j},n}$, and the Burgers vector is collinear with $\hat{\boldsymbol{z}}$. The atom interacts quadratically with neighboring atoms in the same string (the interaction is shown by springs) at $\boldsymbol{r}_{\boldsymbol{j},n\pm1}$. Neighboring atoms in the surrounding strings at $\boldsymbol{r}_{\boldsymbol{j}+\boldsymbol{h},n}$ contribute a periodic sinusoidal interaction, reflecting the periodicity of the lattice described in a mean-field picture. One out of six nearest neighbour string vectors $\boldsymbol{h}$ is shown here.

where m is the atomic mass, α is the spring stiffness between neighboring atoms in the same string, and ω is the periodic interaction strength between atoms in adjacent strings. Below we consider the crystal in a state of elastostatic equilibrium and neglect the kinetic energy term.

The MSFK model contains two unknown force constants α and ω. The linear isotropic elasticity theory also contains two elastic constants, here chosen as Lamé's parameters μ and λ. We can therefore eliminate the unknown force constants by asserting that the model should be consistent with the isotropic elasticity theory. Under the condition that the displacement field varies slowly on the scale comparable with the distance between atoms, the MSFK Lagrangian can be linearized with respect to the strain field, and finally taken to the continuum limit where it is matched to the Lagrangian of the isotropic elasticity theory. This condition is not met in the immediate vicinity of the highly strained dislocation core, but we shall consider it met for the strings that are not immediately adjacent to the glide surface of the dislocation.

The glide surface $\partial\Omega$ separates the crystal lattice into the two bulk regions $\Omega^{\pm}$. Across the glide surface the displacement field is discontinuous because of the plastic slip introduced by the dislocation. The Lagrangian can therefore be represented by a sum of three terms:

$$\mathcal{L} = \mathcal{L}_{\Omega^+} + \mathcal{L}_{\Omega^-} + \mathcal{L}_{\partial\Omega}. \tag{2}$$

By asserting that Lagrangian $\mathcal{L}_{\Omega^\pm}$ in the linear contin-

uum limit must be identical to the Lagrangian of the isotropic elasticity theory, we can match the two unknown force constants of the MSFK model to elastic constants. Through this, the dislocation core properties described by $\mathcal{L}_{\partial\Omega}$ are entirely determined by elastic constants and crystal lattice structure.

Details of the linearization procedure applied to $\mathcal{L}_{\Omega^\pm}$ are given elsewhere [29]. The continuous displacement fields $\boldsymbol{u}^\pm(\boldsymbol{r})$ for $\boldsymbol{r}\in\Omega^\pm$ are introduced as smooth interpolations of atomic displacements according to $\boldsymbol{u}_{n,\boldsymbol{j}} = \boldsymbol{u}^\pm(\boldsymbol{r}_{n,\boldsymbol{j}})$ for $\boldsymbol{r}_{n,\boldsymbol{j}}\in\Omega^\pm$, leading to a continuum form of the MSFK Lagrangian valid in the bulk regions, namely

$$L_{\Omega^\pm} = -\frac{\eta}{2}\int_{\Omega^\pm} \mathrm{d}V\left[\alpha b^2 u_{z,z}^{\pm 2} + m\omega^2 l^2 G\left(u_{z,x}^{\pm 2} + u_{z,y}^{\pm 2}\right)\right], \tag{3}$$

where $u_{i,j} = \partial_j u_i$ is the strain field, and $\eta = 2/a^3$ is the bcc atom number density with lattice constant a. Parameter G stems from the product $h_i h_j = |\boldsymbol{h}|G\delta_{ij} = lG\delta_{ij}$ [30], where $G = 3$ for the hexagonal lattice and $G = 2$ for the square lattice [14], and l is the length of the neighbor vector.

Consider next the Lagrangian of the linear elasticity theory,

$$L_\Omega^{el} = -\frac{1}{2}\int_\Omega \mathrm{d}V\, c_{ijkl}u_{i,j}u_{k,l}, \tag{4}$$

where summation over repeated indices is implied. For the purpose of matching the two models, we only permit displacements in the $\hat{\boldsymbol{z}}$-direction, $u_{i,j} = \delta_{iz}u_{z,j}$, where δ_{ij} is the Kronecker delta symbol. The substitution of the isotropic stiffness tensor $c_{ijkl} = \lambda\delta_{ij}\delta_{kl} + \mu(\delta_{ik}\delta_{jl} + \delta_{il}\delta_{jk})$ leads to

$$L_\Omega^{el} = -\frac{1}{2}\int_\Omega \mathrm{d}V\left[(\lambda+2\mu)u_{z,z}^2 + \mu(u_{z,x}^2 + u_{z,y}^2)\right], \tag{5}$$

where the Cartesian indices are given explicitly and no summation convention is implied. The yet undefined force constants of the MSFK model are matched to elastic constants by equating Eq. (3) to Eq. (5), namely

$$\mu = m\omega^2 l^2 \eta G \tag{6a}$$

$$\lambda = \alpha b^2\eta - 2m\omega^2 l^2 \eta G. \tag{6b}$$

Having identified the force constants, we proceed with defining the glide surface Lagrangian

$$\mathcal{L}_{\partial\Omega} = -\frac{m\omega^2 b^2}{\pi^2}\sum_{\substack{\boldsymbol{j}\in\Omega^+\\ \boldsymbol{j}+\boldsymbol{h}\in\Omega^-}}\sum_{n=-\infty}^{\infty} \sin^2\left\{\frac{\pi}{b}\left[u_z^+(\boldsymbol{r}_{n,\boldsymbol{j}}) - u_z^-(\boldsymbol{r}_{n,\boldsymbol{j}}+\boldsymbol{h})\right]\right\}. \tag{7}$$

where the vector summation is taken only over pairs of strings situated at the opposite sides of the glide surface. The glide surface Lagrangian describes displacement fields $u_z^\pm$ of atomic strings interacting across the plastic slip surface through a non-linear interaction law resulting from (1).

In an earlier study [29], we proceeded under the assumption that the atomic strings that interact non-linearly are situated infinitesimally close to the glide plane, with effectively no separation between them. This approximation leads to an overestimation of the non-linear interaction, and therefore to a highly localized plastic strain field. In other words, the predicted width of the dislocation core is severely underestimated in comparison with atomistic simulations, as we confirm later in Sec. IV. This is a well documented issue associated with applications of the Peierls-Nabarro models based on stacking fault energies to describe non-linear interactions in the core region, which can be rectified through the use of more sophisticated, spatially non-local, functionals of the stacking fault energy [31]. We note that in the earlier study [29] we solved a simpler variation of the boundary value problem which was derived qualitatively, and therefore arrived at a less localized strain field.

In this study we take into account the finite separation between atomic strings in an approximate but analytically tractable manner. The idea is to first solve the problem with strings being infinitesimally close, and subsequently treat the finite separation as a perturbation to the initial solution.

We begin by expressing the glide surface Lagrangian (7) only in terms of the displacement fields at locations very close to the glide surface. Assuming that the glide surface is situated halfway between the string pairs $\boldsymbol{r}_{n,\boldsymbol{j}}$ and $(\boldsymbol{r}_{n,\boldsymbol{j}}+\boldsymbol{h})$, that is at $(\boldsymbol{r}_{n,\boldsymbol{j}}+\frac{1}{2}\boldsymbol{h})$, see Fig. 2, we extrapolate the displacement fields from the string positions towards the glide surface as

$$\begin{aligned} u_z^+(\boldsymbol{r}_{n,\boldsymbol{j}}) &\approx u_z^+(\boldsymbol{r}_{n,\boldsymbol{j}}+\tfrac{1}{2}\boldsymbol{h}) - \tfrac{1}{2}\nabla_{\boldsymbol{h}}u_z^+(\boldsymbol{r}_{n,\boldsymbol{j}}+\tfrac{1}{2}\boldsymbol{h})\\ u_z^-(\boldsymbol{r}_{n,\boldsymbol{j}}+\boldsymbol{h}) &\approx u_z^-(\boldsymbol{r}_{n,\boldsymbol{j}}+\tfrac{1}{2}\boldsymbol{h}) + \tfrac{1}{2}\nabla_{\boldsymbol{h}}u_z^-(\boldsymbol{r}_{n,\boldsymbol{j}}+\tfrac{1}{2}\boldsymbol{h}), \end{aligned} \tag{8}$$

where $\nabla_{\boldsymbol{h}} = h_i\partial_i$ is the directional derivative operator. Using the extrapolation rules given above, Lagrangian (7) can be transformed into an expression compatible with the continuum approximation

$$L_{\partial\Omega} = -\frac{m\omega^2 b}{\pi^2 l}\int_{\partial\Omega}\mathrm{d}S \times\sum_{\boldsymbol{h}\in Neb(\boldsymbol{r})}\sin^2\left\{\frac{\pi}{b}\left[u_z^+ - u_z^- - \tfrac{1}{2}\nabla_{\boldsymbol{h}}\left(u_z^+ + u_z^-\right)\right]\right\}, \tag{9}$$

where the vector summation is performed over the set of strings $Neb(\boldsymbol{r})$, which are the nearest neighbours of a point $\boldsymbol{r}\in\Omega^+$ and lie across the glide surface in Ω^-. The fields are evaluated infinitesimally close to the glide surface in the direction of the surface normal vector. The coordinate dependence of displacement fields in (9) is omitted for brevity.

The above expression gives rise to a complicated boundary value problem for which we have not yet been able to find an analytical solution. Hence we shall first find a solution corresponding to the limit of vanishing

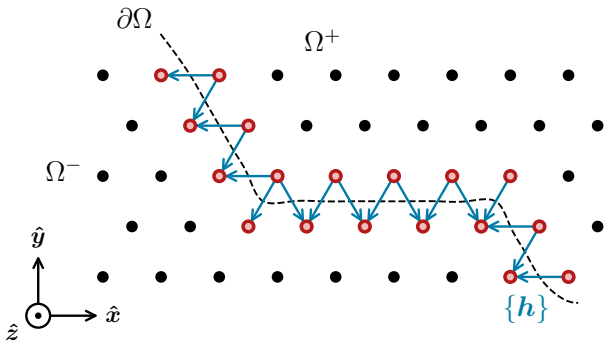

FIG. 2. Bcc lattice viewed in direction collinear with a $a/2[111]$ type Burgers vector. Solid circles represent MSFK strings in a local bulk-like environment, and bordered circles represent the strings adjacent to the glide surface. The glide surface of the continuum model $\partial\Omega$, the cross-section of which is shown by the dashed line, is situated at mid-points of the set of neighbor vectors $\{\boldsymbol{h}\}$ connecting pairs of strings lying at the opposite sides of the glide surface (arrows).

separation between the strings situated at the opposite sides of the glide plane $L^0_{\partial\Omega} = \lim_{\boldsymbol{h}\to 0} L_{\partial\Omega}$. In this case equation (9) reads

$$L^0_{\partial\Omega} = -\mathcal{Z}\frac{m\omega^2 b}{\pi^2 l}\int_{\partial\Omega} \mathrm{d}S\, \sin^2\left[\frac{\pi}{b}\left(u_z^+ - u_z^-\right)\right], \qquad (10)$$

and $\mathcal{Z}$ is the average number of neighbouring strings interacting with a given string across the glide surface. $\mathcal{Z} = 2$ for hexagonal and square lattices, provided that we neglect the curvature of the glide surface at the atomic scale, see Fig. 2.

III. ANALYTICAL SOLUTION FOR THE DISPLACEMENT FIELD OF A STRAIGHT MIXED DISLOCATION

We now proceed to deriving the elastostatic equilibrium equations from the linear elasticity Lagrangian (4) and the simplified glide surface Lagrangian (10). This is accomplished by applying the virtual work principle. The total variation of the Lagrangian is

$$\delta L^0_{\partial\Omega} = \mathcal{Z}\frac{m\omega^2}{\pi l}\int_{\partial\Omega} \mathrm{d}S \sin\left[\frac{2\pi}{b}\left(u_z^+ - u_z^-\right)\right]\left(\delta u_z^- - \delta u_z^+\right). \qquad (11)$$

Similarly, the total variation of the linear elastic Lagrangian (4) is

$$\delta L^{el}_{\Omega^\pm} = \int_{\Omega^\pm} \mathrm{d}V\, c_{ijkl} u^\pm_{k,lj}\delta u^\pm_i - \int_{\partial\Omega} \mathrm{d}S\, c_{ijkl} u^\pm_{k,l} n^\pm_j \delta u^\pm_i \qquad (12)$$

The total variation must vanish at equilibrium in accord with the virtual work principle, namely

$$\delta L^0_{\partial\Omega} + \delta L^{el}_{\Omega^+} + \delta L^{el}_{\Omega^-} = 0. \qquad (13)$$

This results in a boundary value problem of the form

$$c_{ijkl} u^\pm_{k,lj}(\boldsymbol{r}) = 0 \qquad \boldsymbol{r}\in\Omega^\pm \qquad (14a)$$

$$c_{ijkl} u^\pm_{k,l}(\boldsymbol{r}) n^\pm_j(\boldsymbol{r}) = t^\pm_i(\boldsymbol{r}) \qquad \boldsymbol{r}\in\partial\Omega \qquad (14b)$$

where

$$t^\pm_i(\boldsymbol{r}) = \mp\delta_{iz}\mathcal{Z}\frac{m\omega^2}{\pi l}\sin\left[\frac{2\pi}{b}\left(u_z^+(\boldsymbol{r}) - u_z^-(\boldsymbol{r})\right)\right]. \qquad (15)$$

The expression above represents an elastostatic equilibrium problem complemented with traction boundary conditions of the Peierls-Nabarro type for an arbitrarily curved glide surface. We note that an equivalent elastodynamic problem can be formulated by retaining the kinetic energy term in the Lagrangian (1), and using the principle of least action instead.

Consider now the case of a straight dislocation of mixed edge-screw character, lying in the xz-plane with Burgers vector $\boldsymbol{b} \parallel \hat{\boldsymbol{z}}$. Let the dislocation character angle θ represent the angle between the line tangent vector and $\hat{\boldsymbol{y}}$, such that orientations $\theta = 0°$ and $180°$ correspond to pure edge, and $\theta = 90°$ and $270°$ to pure screw dislocations. The outward normal vector to the glide plane is then $n^\pm_j = \mp\delta_{yj}$ and boundary term (14b) for $i = z$ simplifies to

$$c_{zykl} u^\pm_{k,l}(\boldsymbol{r}) = \mathcal{Z}\frac{m\omega^2}{\pi l}\sin\left[\frac{2\pi}{b}\left(u_z^+(\boldsymbol{r}) - u_z^-(\boldsymbol{r})\right)\right]. \qquad (16)$$

Next we substitute the definition of the isotropic stiffness tensor into equation (16)

$$\begin{aligned} c_{zykl} u^\pm_{k,l} &= \left[\lambda\delta_{zy}\delta_{kl} + \mu(\delta_{zk}\delta_{yl} + \delta_{zl}\delta_{yk})\right] u^\pm_{k,l} \\ &= \mu u^\pm_{z,y} + \mu u^\pm_{y,z} \\ &= 2\mu\varepsilon^\pm_{zy}, \end{aligned} \qquad (17)$$

where $\varepsilon_{ij} = \frac{1}{2}(u_{i,j} + u_{j,i})$ is the elastic strain tensor. This leads to the boundary term

$$2\mu\varepsilon^\pm_{zy}(\boldsymbol{r}) = \mathcal{Z}\frac{m\omega^2}{\pi l}\sin\left[\frac{2\pi}{b}\left(u_z^+(\boldsymbol{r}) - u_z^-(\boldsymbol{r})\right)\right]. \qquad (18)$$

Using expressions for the shear modulus (6a) and (6b) derived above, and the dimensionless core structure constant

$$p = \frac{\mathcal{Z}}{2\eta l^3 G}, \qquad (19)$$

we collate the constants and arrive at the final expression

$$\frac{\pi}{p}\varepsilon^\pm_{zy}(\boldsymbol{r}) = \sin\left[\frac{2\pi}{b}\left(u_z^+(\boldsymbol{r}) - u_z^-(\boldsymbol{r})\right)\right]. \qquad (20)$$

Summarizing, the boundary value problem for a flat glide plane is defined by equations

$$c_{ijkl} u^\pm_{k,lj} = 0, \qquad \boldsymbol{r}\in\Omega^\pm \qquad (21a)$$

$$\varepsilon^\pm_{xy} = 0, \qquad \boldsymbol{r}\in\partial\Omega \qquad (21b)$$

$$\varepsilon^\pm_{yy} = 0, \qquad \boldsymbol{r}\in\partial\Omega \qquad (21c)$$

$$\frac{\pi}{p}\varepsilon^\pm_{zy} = \sin\left[\frac{2\pi}{b}\left(u_z^+ - u_z^-\right)\right], \qquad \boldsymbol{r}\in\partial\Omega \qquad (21d)$$

The substitution of the core structure constant (19) also results in a more compact notation for the glide plane Lagrangian (10)

$$L^0_{\partial\Omega} = -\frac{2\mu bp}{\pi^2}\int_{\partial\Omega} \mathrm{d}S\, \sin^2\left[\frac{\pi}{b}\left(u_z^+ - u_z^-\right)\right]. \tag{22}$$

Now we focus on solving the boundary value problem defined by Eqns. (21) above. The singular Volterra displacement field $u_i^v(\boldsymbol{r})$, which can be obtained from the Burgers displacement formula [2], simultaneously satisfies the elastostatic equilibrium condition (21a) and the two traction-free conditions (21b) and (21c), with the exception of the points where the strain field is divergent. We can hence solve the combined boundary value problem (21) by convolving the Volterra field with a non-singular distribution function. This distribution function removes the divergence of the singular Volterra field, and must be chosen such that the non-linear traction condition (21d) is met. The traction-free and elastostatic conditions remain satisfied because taking a partial derivative or performing a convolution are linear operations, both acting on the displacement field.

We find an exact solution for the strain field of a straight mixed dislocation by convolving the Volterra displacement field with a Cauchy-Lorentzian distribution

$$u_i(x,y,z) = \int_{-\infty}^{\infty} \mathrm{d}s\, \rho(s-z) u_i^v(x,y,s), \tag{23}$$

where

$$\rho(s) = \frac{1}{\pi\kappa}\left(\frac{\kappa^2}{s^2+\kappa^2}\right) \tag{24}$$

is the Cauchy-Lorentzian distribution with width $\kappa > 0$, where the latter depends on the dislocation character. The above convolution approach exemplifies the link between the Peierls-Nabarro and Lubarda-Markenscoff variable core dislocation models [15, 32].

A full analytical solution describing the MSFK displacement field of a dislocation is given in the Appendix. The solution shows that the width of the core κ increases at $\theta \to 90°$ or $270°$ or, in other words, as the screw character of the dislocation becomes more dominant:

$$\kappa(\theta) = \frac{b}{8p\sqrt{1+\tan^2\theta}}\left(\frac{1}{1-\nu} + \tan^2\theta\right). \tag{25}$$

The solution satisfies all the conditions of the boundary value problem (21). For $\theta \to 0°$ or $180°$ the solution reduces to the known form, describing a straight edge dislocation [16, 29, 33].

IV. CORE BROADENING DUE TO FINITE INTERATOMIC SEPARATION EFFECTS AT THE GLIDE PLANE

We now consider a perturbation approach, to correct the above result for the finite separation between string pairs lying adjacent to the glide plane. First, we rewrite the glide plane Lagrangian (9) using the displacement field symmetry relations $u_z^+ - u_z^- = 2u_z^+$ and $u_{z,y}^+ = u_{z,y}^-$, see Appendix A. Furthermore, we take h_x and h_z components as zeros, as their absolute values are significantly smaller than h_y. The resulting solution depends solely on the elevation of atomic strings above or under the glide plane $h = |h_y| = |\boldsymbol{h}\cdot\hat{\boldsymbol{y}}|$, namely

$$L_{\partial\Omega} = -\frac{2\mu bp}{\pi^2}\int_{\partial\Omega} \mathrm{d}S\, \sin^2\left[\frac{\pi}{b}\left(2u_z^+ + hu_{z,y}^+\right)\right]. \tag{26}$$

We see that the effect of the glide plane elevation h softens the role of disregistry, leading to a solution with a broader core. It is desirable to express this effect as an approximate scaling law for an effective core structure constant $p_h \leq p$ that we can apply to the analytical solution found for the $h \to 0$ limit above. This is a minimization problem: we seek to find an effective structure constant p_h that most closely captures the core broadening as a function of h. Assuming that the glide plane Lagrangian provides a reliable measure of the core width, we recast the problem in terms of a condition on the Lagrangian

$$L^0_{\partial\Omega}(p_h) = L_{\partial\Omega}(p). \tag{27}$$

In effect, we seek to find a scaled core structure constant p_h, for which the energy of the unperturbed solution is equal to the energy of the perturbed system. We use the analytical expression for the displacement field found above in the limit $h \to 0$ in both cases, which could be considered as the first step in a self-consistent solution scheme. Owing to the already approximate nature of the approach taken so far, there is little reason to go beyond this first-order approximate step.

First we evaluate the unperturbed Lagrangian $L^0_{\partial\Omega}(p_h)$ (22), using the expression for the displacement field in the near vicinity of the glide plane (A5c):

$$\begin{aligned} L^0_{\partial\Omega}(p_h) &= c\int_{\partial\Omega} \mathrm{d}S\, \sin^2\left(\frac{2\pi}{b}u_z^+\right) \\ &= cl_x\int_{-\infty}^{\infty} \mathrm{d}z\, \frac{\kappa_h^2}{\kappa_h^2+z^2} \\ &= cl_x\pi\kappa_h, \end{aligned} \tag{28}$$

where l_x is the dislocation length in the x direction, and κ_h is the dislocation core width (25), but with p replaced with the yet unknown parameter p_h. Prefactor c is introduced for brevity, where $c = -2\mu bp/\pi^2$. Similarly, we evaluate the perturbed Lagrangian $L_{\partial\Omega}(p)$ defined in Eq. (26), using the expression for the strain field in the vicinity of the glide plane (A6b):

$$\begin{aligned} L_{\partial\Omega}(p) &= c\int_{\partial\Omega} \mathrm{d}S\, \sin^2\left[\frac{\pi}{b}\left(2u_z^+ + hu_{z,y}^+\right)\right] \\ &\approx cl_x\pi\kappa + \frac{cl_x\pi h}{2\sqrt{1+\tan^2\theta}}\left(\frac{3-2\nu}{2-2\nu} + \tan^2\theta\right), \end{aligned} \tag{29}$$

TABLE I. Structure constant p (dimensionless) and the dislocation core width κ (in Å units) shown as functions of the dislocation character. We give the values of the core width without the height correction $\kappa(\theta)$, with the height correction $\kappa_h(\theta)$, and with the approximate height correction $\kappa_{h'}(\theta)$, respectively, using the structure constants from Eqs. (19), (30), and (31). The dislocation core width diverges as $\theta \to \pm 90°$.

angle θ (°)	p	$p_h(\theta)$	$\kappa(\theta)$	$\kappa_h(\theta)$	$\kappa_{h'}(\theta)$
0 (pure edge)	0.306	0.138	1.54	3.42	3.42
15	0.306	0.139	1.57	3.46	3.48
30	0.306	0.140	1.66	3.61	3.68
45	0.306	0.144	1.88	3.99	4.16
60	0.306	0.148	2.44	5.04	5.41
75	0.306	0.152	4.40	8.89	9.77
90 (screw)	0.306	0.153	∞	∞	∞

where we have performed a series expansion in h at 0 to first order to obtain an analytically solvable integral. Equating expressions (28) and (29) enables solving for the perturbed structure constant p_h:

$$p_h(\theta) = \frac{bp\left(1-\nu\sin^2\theta\right)}{2hp\left[(3-2\nu)-\sin^2\theta\right]+b(1-\nu\sin^2\theta)}. \quad (30)$$

In Table I we give values of the perturbed structure constant p_h and the corresponding core width κ_h for a range of dislocation character angles θ. Material parameters are chosen appropriately for the $a/2[111](10\bar{1})$ edge dislocation in bcc tungsten, where $p = \sqrt{3}/(4\sqrt{2})$, $h = a/\sqrt{2}$, $b = \sqrt{3}a/2$, $\nu = 0.28$, and $a = 3.14\,\text{Å}$. We find that the core width effectively doubles as a result of the height correction. Notably, the angular dependence of $p_h(\theta)$ has a minor effect on the core width and may therefore be neglected, leading to a simplified expression for the perturbed structure constant:

$$p_h(\theta) \approx p_h(0) = \frac{bp}{b+2hp(3-2\nu)}. \quad (31)$$

In conclusion, above we derived an approximate analytical expression describing the broadening of the dislocation core due to the finite separation between atoms at the glide plane. The effect of broadening is substantial for a straight mixed dislocation, and must be taken into account to describe displacement fields in better agreement with atomistic simulations. Atomic displacement fields derived from molecular dynamics simulations and analytical solutions are compared below.

V. COMPARISON OF ANALYTICAL SOLUTIONS AND ATOMISTIC SIMULATIONS

The continuum displacement fields derived from analytical solutions given above are compared to the data derived directly from atomistic simulations performed using the LAMMPS [34] molecular dynamics program. We simulate a mixed tungsten dislocation dipole of $a/2[111](\bar{1}01)$ type using the embedded-atom model potential by Marinica *et al.* [35].

The simulation cell was initialized with a pristine bcc lattice oriented along the basis set $\boldsymbol{x} = \frac{2}{3}[1\bar{2}1]$, $\boldsymbol{y} = [\bar{1}01]$, and $\boldsymbol{z} = [111]$ in the units of lattice parameter a. Periodic boundary conditions were applied in all three directions, and the simulation cell vectors were chosen as

$$\begin{aligned} \boldsymbol{c}_{\boldsymbol{x}} &= n_x\boldsymbol{x} + n_k\boldsymbol{k} \\ \boldsymbol{c}_{\boldsymbol{y}} &= n_y\boldsymbol{y} \\ \boldsymbol{c}_{\boldsymbol{z}} &= n_z\boldsymbol{z}. \end{aligned} \quad (32)$$

The kink vector $n_k\boldsymbol{k}$ causes the cell to acquire a triclinic shape, thus forcing the dislocation tangent vectors to be collinear with $\boldsymbol{c}_{\boldsymbol{x}}$, while the Burgers vector remains at $\boldsymbol{b} = a/2[111]$ and the glide plane remains parallel to the xz-plane. The dislocations increasingly acquire the screw character as n_k increases. For $n_k = 0$ this setup reduces to an orthogonal cell, and for $n_k = 1$ it reduces to single-kink boundary conditions [21, 36].

To generate displacement fields suitable for comparison with analytical solutions given above, we initialized a dipole of mixed $a/2[111](\bar{1}01)$ dislocations with $\boldsymbol{k} = \boldsymbol{b}$. We refer to Fig. 3 for a sketch of the geometry used in atomistic simulations.

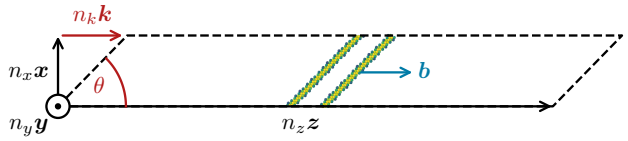

FIG. 3. Triclinic simulation cell (dashed line) containing a dipole of mixed dislocations inclined at a character angle of θ, as seen looking along the $-\boldsymbol{y}$ direction. The coordinate system is defined in Eq. (32). The Burgers vector is not drawn to scale.

We chose the cell dimensions of $(n_x, n_y, n_z) = (15, 34, 99)$. An additional half-plane of atoms was introduced to enable the formation of a dislocation dipole, leading to a simulation involving 405000 atoms in the cell. The dislocation dipole was initialized by displacing atoms according to the Volterra displacement field of a mixed dislocation dipole. We used a relaxation procedure consisting of three steps for the purpose of escaping shallow energy minima. First, the atomic configuration was relaxed statically. Subsequently, the system was annealed at a temperature of 900 K for 5 ps, before the final static relaxation. This setup was repeated over a broad range of n_k values, spanning an interval of dislocation character angles θ from 0° to 85°.

Atomic strains $u_{z,z}$ were extracted along atomic rows collinear to $\boldsymbol{b}$, for the atomic rows immediately above and below a dislocation glide plane.

We found the atomic strains to be stacked in symmetric (a) and asymmetric (b) configurations in alternating order. An explanation for this effect is that atomic planes alternate in height along the $[1\bar{2}1]$ direction, such that the

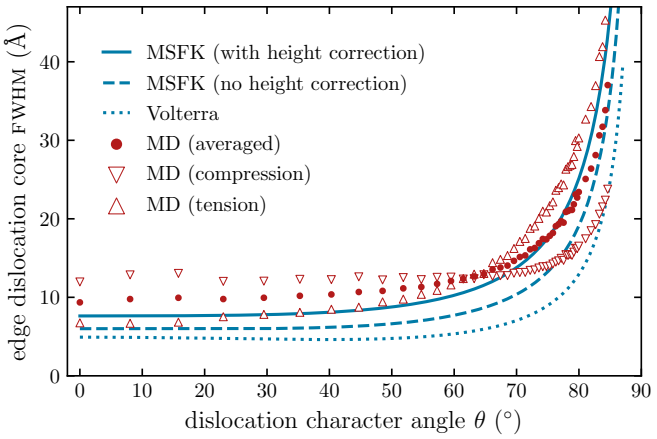

FIG. 4. Dislocation core width plotted as a function of the dislocation character angle, measured as the full width at half maximum (FWHM) along the Burgers vector direction. The molecular dynamics (MD) core widths are extracted from the first atomic rows immediately above or below the glide plane, which are under compression or tension, respectively.

apparent glide plane position in (a) is centered between atomic rows under compression and tension, while in (b) it is significantly closer to the atomic row under tension [29].

Atomistic dislocation core widths are measured from the full-width at half maximum (FWHM) of Lorentzian distributions fitted to the atomistic strain field. Similarly, continuum dislocation core widths are extracted by fitting Lorentzian distributions to the analytical $u_{z,z}$ strain field given by Eq. (A4) evaluated at an offset of h in the y direction, consistent with the average height of atomic rows above or below the glide plane. This process is repeated for three types of continuum models, listed below in the order of ascending accuracy:

1. Volterra, $p \to 0$
2. MSFK, without height correction, $p = \sqrt{3}/(4\sqrt{2})$
3. MSFK, with height correction, p_h from Eq. (30)

In Fig. 4 we compare the atomistic dislocation core widths to predictions derived from the continuum model over an interval of dislocation character angles θ. We show the core widths of the atomically computed tensile or compressive fields averaged over the two stacking configurations, as well as an overall averaged value. Comparisons show that the Volterra model consistently underestimates the dislocation core widths by about 50% on average. This is expected, as the Volterra strain field diverges at the dislocation core. The MSFK model without the height correction shows improved agreement, but the predicted core widths are still underestimated on average by about 30%. In contrast, the MSFK model, including the height correction, yields the dislocation core widths within 10% to 20% agreement to the average atomistic core widths over the entire range of character angles.

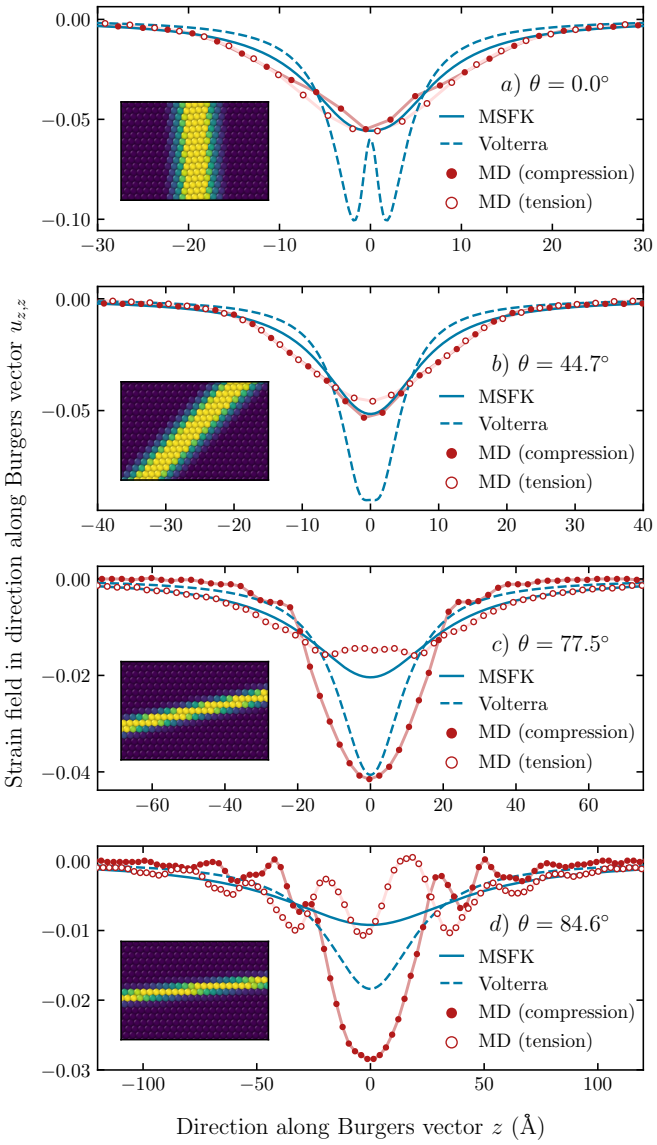

FIG. 5. Comparison between the strain fields derived from molecular dynamics (MD) and predicted by the MSFK and Volterra continuum models for the $a/2[111](10\bar{1})$ mixed dislocation in tungsten at a few selected dislocation angles. The strain of the atomic row under tension is plotted with negative sign. The atomistic structure (inset), colored according to the potential energy of atoms and seen in the normal direction to the glide plane, reveals the formation of kinks at large dislocation character angles.

The interpretation of atomistic core widths involves an element of subtlety. The strain field in the dislocation core exhibits a strong degree of asymmetry between the regions that are under compressive and tensile stresses. It is partially a feature of atomic bonding; for a crystal lattice under an equal amount of compressive or tensile stress, the absolute tensile strain is greater than the absolute compressive strain. A strongly peaked strain field translates to a more compact dislocation core, consequently one would expect the dislocation core under

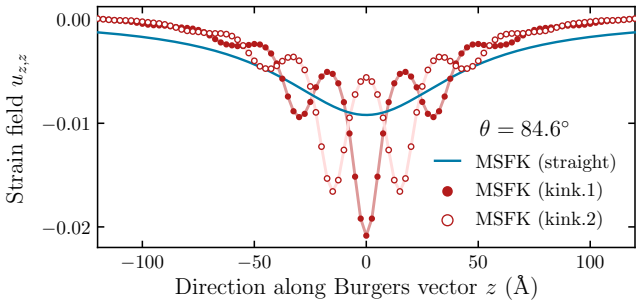

FIG. 6. MSFK prediction of the strain field assuming a mixed dislocation with staircase line shape (dotted), as an approximation to the kinked line found in atomistic simulations. Pictured here are the strain fields of two kinked lines centered at differing points, see the main text. The MSFK prediction exhibits a similar substructure to the atomistic strain field at equivalent inclination, providing a clear evidence of kink formation.

tension to be narrower. This is indeed the case for character angles of $\theta \lessapprox 65°$, as is readily seen in Fig. 4. At larger character angles inversion occurs, and the dislocation core under compression becomes narrower. To explain this finding, we need to take a closer look at the strain fields computed atomistically.

In Fig. 5 we show plots of the core strain fields derived from atomistic simulations and continuum models for a few selected dislocation character angles. The strain field derived from atomistic simulations at low angles is in excellent agreement with the MSFK continuum model. For the angles above $\theta \approx 60°$ the effect of kinks becomes more pronounced; an internal substructure of multiple peaks appears as the separation between the kinks increases, see the inset in Fig. 5. As the kinks become well separated, most of the dislocation line locally acquires the pure screw character, with short edge dislocation segments connecting straight screw dislocation segments [37]. The dislocation line does not acquire a mixed character uniformly, and hence the continuum model description assuming a straight mixed dislocation line becomes invalid.

Fig. 6 shows the continuum strain field of a dislocation line where kinks have been introduced deliberately in the form of a staircase, assuming the kink height of $\sqrt{2/3}a = 2.56\,\text{Å}$ and kink separation of 27 Å to yield the average dislocation character angle of $\theta = 84.6°$. The approximate MSFK strain field was obtained from a numerical convolution of the Volterra model strain field with a Lorentzian kernel with an *ad-hoc* width $\kappa_h(\theta = 60°) = 5\,\text{Å}$. The strains labeled as kink.1 or kink.2 are computed from dislocations centered at a kink or at a screw-segment midpoint, respectively. The resulting strain fields show a characteristic substructure similar to that of the atomistic strain fields, providing evidence that the substructure can be readily explained by the effect of formation of kinks.

We note that the strain fields computed using the approximate form for p_h given by Eq. (31) are practically indistinguishable from the character-dependent height correction that uses p_h from Eq. (30). We therefore recommend using the approximate expression and take advantage of its simplicity.

VI. CONCLUSION

We have derived a continuum model for the straight dislocation of mixed character in a bcc lattice. We found an exact analytical solution for the strain field of an arbitrary mixed dislocation, which is non-singular and is valid in the entire space including the core region, and which satisfies both the elastostatic equilibrium condition and the Peierls-Nabarro traction condition. We emphasize that the continuum model is based on a simple description of the periodic crystal lattice and is free from adjustable parameters.

The shape and the width of the strain field in the core region of a dislocation is in agreement with atomistic reference simulations performed for a mixed $a/2[111](\bar{1}01)$ dislocation in tungsten over a broad interval of dislocation character angles from $\theta = 0°$ up to approximately $\theta = 60°$. At larger character angles, atomistic simulations predict the formation of well separated kinks, and this invalidates the representation of a dislocation as a straight linear object. Nevertheless, the average width of the dislocation core predicted by analytical solution remains consistent with the atomistic simulations, confirming the validity of the solution and its suitability for a coarse-grained description of the dislocation core.

ACKNOWLEDGMENTS

This work has been carried out within the framework of the EUROfusion Consortium and has received funding from the Euratom research and training programme 2014-2018 and 2019-2020 under Grant Agreements No. 633053 and No. 755039. Also, it has been partially funded by the RCUK Energy Programme (Grant No. EP/P012450/1). The views and opinions expressed herein do not necessarily reflect those of the European Commission. Useful discussions with Andrew J. London and Daniel R. Mason are gratefully acknowledged.

Appendix A: Analytical solution

Below we give an analytical solution to the displacement field of a straight mixed dislocation, and explore some limiting cases given in the main part of the paper.

We start by defining the following coordinate transfor-

mations

$$\begin{aligned} m &= \tan\theta \\ y_m &= \sqrt{1+m^2}\,y \\ z_m &= z - mx \end{aligned} \tag{A1}$$

that provide the more compact notation required for the presentation of the analytical formulae below. The displacement field of a mixed straight dislocation with Burgers vector $\boldsymbol{b} \parallel \hat{\boldsymbol{z}}$ has the form

$$u_x^{\pm}(\boldsymbol{r}) = -\frac{b}{4\pi(1-\nu)(1+m^2)}\left(\frac{m y_m z_m[z_m^2+(y_m\mp\kappa)^2]}{(y_m^2+z_m^2+\kappa^2)^2-4y_m^2\kappa^2}\right) \tag{A2}$$

$$u_y^{\pm}(\boldsymbol{r}) = \frac{b}{8\pi(1-\nu)\sqrt{1+m^2}}\left(\sqrt{1+m^2} - 2\frac{\left[z_m^2+(y_m\mp\kappa)^2\right]\left[z_m^2+\kappa(\kappa\pm y_m)\right]}{(y_m^2+z_m^2+\kappa^2)^2-4y_m^2\kappa^2} - (1-2\nu)\ln\left[z_m^2+(y_m\pm\kappa)^2\right]\right) \tag{A3}$$

$$u_z^{\pm}(\boldsymbol{r}) = \pm\frac{b}{4} + \frac{b}{4\pi(1-\nu)(1+m^2)}\left(\frac{y_m z_m[z_m^2+(y_m\mp\kappa)^2]}{(y_m^2+z_m^2+\kappa^2)^2-4y_m^2\kappa^2}\right) - \frac{b}{2\pi}\arctan\left(\frac{z_m}{y_m\pm\kappa}\right), \tag{A4}$$

where u_i^+ is valid for $y>0$, and u_i^- is valid for $y<0$. The displacement fields are defined in the limit where the coordinates are close to the glide plane, namely

$$\lim_{y\to 0^{\pm}} u_x^{\pm}(\boldsymbol{r}) = 0 \tag{A5a}$$

$$\lim_{y\to 0^{\pm}} u_y^{\pm}(\boldsymbol{r}) = \frac{b\left[\sqrt{1+m^2}-2-(1-2\nu)\ln\left(z_m^2+\kappa^2\right)\right]}{8\pi(1-\nu)\sqrt{1+m^2}} \tag{A5b}$$

$$\lim_{y\to 0^{\pm}} u_z^{\pm}(\boldsymbol{r}) = \pm\frac{b}{4\pi}\left[\pi - 2\arctan\left(\frac{z_m}{\kappa}\right)\right]. \tag{A5c}$$

The strain fields in the vicinity of the glide plane are also well-defined, for example the u_z components of the strain field are

$$\lim_{y\to 0^{\pm}} u_{z,x}^{\pm}(\boldsymbol{r}) = \pm\frac{bm\kappa}{2\pi\left(z_m^2+\kappa^2\right)} \tag{A6a}$$

$$\lim_{y\to 0^{\pm}} u_{z,y}^{\pm}(\boldsymbol{r}) = \frac{bz_m\left[2(1+m^2)+(1-\nu)^{-1}\right]}{4\pi\sqrt{1+m^2}(z_m^2+\kappa^2)} \tag{A6b}$$

$$\lim_{y\to 0^{\pm}} u_{z,z}^{\pm}(\boldsymbol{r}) = \mp\frac{b\kappa}{2\pi\left(z_m^2+\kappa^2\right)}. \tag{A6c}$$

Solution of the boundary value problem also involves the $u_{y,z}$ strain component in the limit approaching the glide plane:

$$\lim_{y\to 0^{\pm}} u_{y,z}^{\pm}(\boldsymbol{r}) = \frac{bz_m\left[(1-\nu)^{-1}-2\right]}{4\pi\sqrt{1+m^2}(z_m^2+\kappa^2)}. \tag{A7}$$

Finally, the width of the dislocation core, as shown by Eq. (25), is obtained by substituting the $u_z^{\pm}$ component of the displacement field (A5c) and the $u_{z,y}^{\pm}$ and $u_{y,z}^{\pm}$ strain fields (A6b) and (A7) into the boundary value problem (21d), subsequently solving them for $\kappa(\theta)$.

[1] T. Mura, *Micromechanics of defects in solids* (Springer Science & Business Media, 2013).
[2] P. M. Anderson, J. P. Hirth, and J. Lothe, *Theory of Dislocations* (Cambridge University Press, 2017).
[3] V. Volterra, "Sur l'équilibre des corps élastiques multiplement connexes," in *Annales scientifiques de l'École normale supérieure*, Vol. 24 (1907) pp. 401–517.
[4] R. Peierls, "The size of a dislocation," Proceedings of the Physical Society **52**, 34 (1940).
[5] F. R. N. Nabarro, "Dislocations in a simple cubic lattice," Proceedings of the Physical Society **59**, 256 (1947).
[6] G. Schoeck, "The Peierls model: progress and limitations," Materials Science and Engineering: A **400**, 7–17 (2005).
[7] Y. Zhang and A. H. W. Ngan, "Dislocation-density dynamics for modeling the cores and Peierls stress of curved dislocations," International Journal of Plasticity **104**, 1–22 (2018).
[8] V. V. Bulatov and E. Kaxiras, "Semidiscrete variational peierls framework for dislocation core properties," Physical Review Letters **78**, 4221 (1997).
[9] H. Wei, Y. Xiang, and P. Ming, "A generalized Peierls-Nabarro model for curved dislocations using discrete Fourier transform," Communications in computational

physics **4**, 275–293 (2008).
[10] G. Liu, X. Cheng, J. Wang, K. Chen, and Y. Shen, "Atomically informed nonlocal semi-discrete variational Peierls-Nabarro model for planar core dislocations," Scientific Reports **7**, 43785 (2017).
[11] B. A. Szajewski, A. Hunter, and I. J. Beyerlein, "The core structure and recombination energy of a copper screw dislocation: a Peierls study," Philosophical Magazine **97**, 2143–2163 (2017).
[12] W. Cai, A. Arsenlis, C. R. Weinberger, and V. V. Bulatov, "A non-singular continuum theory of dislocations," Journal of the Mechanics and Physics of Solids **54**, 561–587 (2006).
[13] G. Po, M. Lazar, D. Seif, and N. Ghoniem, "Singularity-free dislocation dynamics with strain gradient elasticity," Journal of the Mechanics and Physics of Solids **68**, 161–178 (2014).
[14] S. L. Dudarev, "Coherent motion of interstitial defects in a crystalline material," Philosophical Magazine **83**, 3577–3597 (2003).
[15] V. A. Lubarda and X. Markenscoff, "Variable core model and the peierls stress for the mixed (screw-edge) dislocation," Applied physics letters **89**, 151923 (2006).
[16] V. A. Lubarda and X. Markenscoff, "Configurational force on a lattice dislocation and the Peierls stress," Archive of Applied Mechanics **77**, 147–154 (2007).
[17] L. Ventelon, F. Willaime, E. Clouet, and D. Rodney, "Ab initio investigation of the Peierls potential of screw dislocations in bcc Fe and W," Acta Materialia **61**, 3973–3985 (2013).
[18] L. Dezerald, L. Ventelon, E. Clouet, C. Denoual, D. Rodney, and F. Willaime, "Ab initio modeling of the two-dimensional energy landscape of screw dislocations in bcc transition metals," Physical Review B **89**, 024104 (2014).
[19] L. Dezerald, D. Rodney, E. Clouet, L. Ventelon, and F. Willaime, "Plastic anisotropy and dislocation trajectory in bcc metals," Nature Communications **7**, 11695 (2016).
[20] A. H. W. Ngan, "A generalized Peierls-Nabarro model for nonplanar screw dislocation cores," Journal of the Mechanics and Physics of Solids **45**, 903–921 (1997).
[21] E. Clouet, L. Ventelon, and F. Willaime, "Dislocation core energies and core fields from first principles," Physical review letters **102**, 055502 (2009).
[22] E. Clouet, "Elastic energy of a straight dislocation and contribution from core tractions," Philosophical Magazine **89**, 1565–1584 (2009).
[23] E. Clouet, "Dislocation core field. I. modeling in anisotropic linear elasticity theory," Physical Review B **84**, 224111 (2011).
[24] S. Chiesa, M. R. Gilbert, S. L. Dudarev, P. M. Derlet, and H. Van Swygenhoven, "The non-degenerate core structure of a $1/2\langle 111\rangle$ screw dislocation in bcc transition metals modelled using Finnis–Sinclair potentials: The necessary and sufficient conditions," Philosophical Magazine **89**, 3235–3243 (2009).
[25] M. R. Gilbert and S. L. Dudarev, "Ab initio multi-string Frenkel–Kontorova model for a $b = a/2[111]$ screw dislocation in bcc iron," Philosophical Magazine **90**, 1035–1061 (2010).
[26] M. R. Gilbert, *BCC metals in extreme environments: Modelling the structure and evolution of defects*, Ph.D. thesis, Oxford University, UK (2010).
[27] P. M. Derlet, D. Nguyen-Manh, and S. L. Dudarev, "Multiscale modeling of crowdion and vacancy defects in body-centered-cubic transition metals," Physical Review B **76**, 054107 (2007).
[28] S. L. Dudarev, "The non-Arrhenius migration of interstitial defects in bcc transition metals," Comptes Rendus Physique **9**, 409–417 (2008).
[29] M. Boleininger, T. D. Swinburne, and S. L. Dudarev, "Atomistic-to-continuum description of edge dislocation core: Unification of the Peierls-Nabarro model with linear elasticity," Phys. Rev. Materials **2**, 083803 (2018).
[30] In a previous derivation [29] the summation was restricted to only consider neighboring strings within the integration domains Ω^+ or Ω^-. This distinction is not necessary in the continuum limit as surface effects will already be captured as tractions upon application of the variational principle.
[31] G. Liu, X. Cheng, J. Wang, K. Chen, and Y. Shen, "Improvement of nonlocal Peierls-Nabarro models," Computational Materials Science **131**, 69–77 (2017).
[32] C. L. Hall and X. Markenscoff, "On approaches to modelling lattice dislocations," Philosophical Magazine Letters (2011).
[33] M. Lazar, "Non-singular dislocation continuum theories: strain gradient elasticity vs. Peierls–Nabarro model," Philosophical Magazine **97**, 3246–3275 (2017).
[34] S. Plimpton, "Fast parallel algorithms for short-range molecular dynamics," Journal of computational physics **117**, 1–19 (1995).
[35] M.-C. Marinica, L. Ventelon, M. R. Gilbert, L. Proville, S. L. Dudarev, J. Marian, G. Bencteux, and F. Willaime, "Interatomic potentials for modelling radiation defects and dislocations in tungsten," Journal of Physics: Condensed Matter **25**, 395502 (2013).
[36] T. D. Swinburne, S. L. Dudarev, S. P. Fitzgerald, M. R. Gilbert, and A. P. Sutton, "Theory and simulation of the diffusion of kinks on dislocations in bcc metals," Physical Review B **87**, 064108 (2013).
[37] K. Kang, V. V. Bulatov, and W. Cai, "Singular orientations and faceted motion of dislocations in body-centered cubic crystals," Proceedings of the National Academy of Sciences **109**, 15174–15178 (2012).